ORIGINAL ARTICLE

Real-Time Magnetic Resonance Imaging
Radial Gradient-Echo Sequences With Nonlinear Inverse Reconstruction

Jens Frahm, PhD,*† Dirk Voit, PhD,* and Martin Uecker, PhD†‡

Objective: The aim of this study is to evaluate a real-time magnetic resonance imaging (MRI) method that not only promises high spatiotemporal resolution but also practical robustness in a wide range of scientific and clinical applications.
Materials and Methods: The proposed method relies on highly undersampled gradient-echo sequences with radial encoding schemes. The serial image reconstruction process solves the true mathematical task that emerges as a nonlinear inverse problem with the complex image and all coil sensitivity maps as unknowns. Extensions to model-based reconstructions for quantitative parametric mapping further increase the number of unknowns, for example, by adding parameters for phase-contrast flow or T1 relaxation. In all cases, an iterative numerical solution that minimizes a respective cost function is achieved with use of the iteratively regularized Gauss-Newton method. Convergence is supported by regularization, for example, to the preceding frame, whereas temporal fidelity is ensured by downsizing the regularization strength in comparison to the data consistency term in each iterative step. Practical implementations of highly parallelized algorithms are realized on a computer with multiple graphical processing units. It is "invisibly" integrated into a commercial 3-T MRI system to allow for conventional usage and to provide online reconstruction, display, and storage of regular DICOM image series.
Results: Depending on the application, the proposed method offers serial imaging, that is, the recording of MRI movies, with variable spatial resolution and up to 100 frames per second (fps)—corresponding to 10 milliseconds image acquisition times. For example, movements of the temporomandibular joint during opening and closing of the mouth are visualized with use of simultaneous dual-slice movies of both joints at 2 × 10 fps (50 milliseconds per frame). Cardiac function may be studied at 30 to 50 fps (33.3 to 20 milliseconds), whereas articulation processes typically require 50 fps (20 milliseconds) or orthogonal dual-slice acquisitions at 2 × 25 fps (20 milliseconds). Methodological extensions to model-based reconstructions achieve improved quantitative mapping of flow velocities and T1 relaxation times in a variety of clinical scenarios.
Conclusions: Real-time gradient-echo MRI with extreme radial undersampling and nonlinear inverse reconstruction allows for direct monitoring of arbitrary physiological processes and body functions. In many cases, pertinent applications offer hitherto impossible clinical studies (eg, of high-resolution swallowing dynamics) or bear the potential to replace existing MRI procedures (eg, electrocardiogram-gated cardiac examinations). As a consequence, many novel opportunities will require a change of paradigm in MRI-based radiology. At this stage, extended clinical trials are needed.

The ability to perform magnetic resonance imaging (MRI) examinations in real time solves a variety of problems in routine diagnostic imaging. In particular, real-time MRI simplifies and accelerates established procedures, adds completely new possibilities, and even promises to reduce costs when leading to shorter examination times and less failures due to motion problems. For these reasons, and based on recent technical progress in hardware and software, real-time MRI becomes a realistic challenge. Principle approaches either exploit the ability of rapid gradient-echo sequences to continuously acquire data in a steady-state situation[1] or adopt the intrinsic speed of single-shot methods such as echo-planar imaging[2] or spiral imaging.[3] Technically, all recent attempts toward acceleration also benefit from data undersampling, multicoil acquisitions, and the concept of parallel imaging.[4,5]

The present work focuses on the development of a specific real-time MRI method that aims to combine an optimized acquisition strategy with a proper mathematical solution of the resulting image reconstruction problem. The proposed technique offers high image quality at unsurpassed temporal resolution.[6] It uses strongly undersampled gradient-echo sequences with radial encoding schemes and correctly treats serial image reconstruction as a nonlinear inverse problem with suitable regularization. In practice, the approach is not only robust but also easy to use. This is because online reconstruction and display of real-time images may be accomplished by upgrading a commercial MRI system with a highly parallelized algorithm that runs on an integrated "bypass" computer equipped with multiple graphical processing units (GPUs).

The primary aim of this contribution is to evaluate the general utility of the proposed real-time MRI method in science and medicine. This is accomplished by demonstrating the achievable image quality, presenting possible applications, and describing extensions toward quantitative parametric mapping. Although preliminary patient studies document clinical usefulness in a number of fields, the purpose of the present work is best served by studies of healthy subjects to initiate large-scale clinical trials.

MATERIALS AND METHODS

All studies were performed at 3 T using an MRI system with 80 mT·m^{-1} gradients (Magnetom Prisma; Siemens Healthineers, Erlangen, Germany). However, to ensure optimal subject compliance, all real-time MRI sequences used below-maximum slew rates to avoid peripheral nerve stimulation under all circumstances. Depending on the application, examinations used the standard 64-channel head coil or combinations of the 18-channel thorax coil with selected elements of the spine coil array. Dynamic studies of the temporomandibular joint (TMJ) and hand were performed with use of dedicated 15-channel and 16-channel radiofrequency coils (NORAS MRI Products, Hochberg, Germany), respectively.

This study recruited young healthy subjects without known illness. Written informed consent, according to the recommendations of the local ethics committee, was obtained before MRI. Moreover, all examinations were performed with radiofrequency spoiled FLASH MRI sequences,[7] yielding T1 or spin-density contrast as controlled by the flip angle. Because of the very short echo times for real-time imaging,

Frahm et al

Investigative Radiology • Volume 54, Number 12, December 2019

almost all applications were accomplished without additional shimming using tune-up field homogeneity conditions. The resulting serial images neither suffer from signal void or geometric distortions due to magnetic field inhomogeneities nor reveal banding artifacts as typically seen for balanced steady-state free precession (SSFP) acquisitions. A list of acquisition parameters for real-time MRI applications established here is given in Table 1.

In general, however, because the real-time MRI technique relies on a generic gradient-echo sequence, applications are possible with all common contrasts: spoiled FLASH, refocused FLASH, balanced SSFP, and reverse SSFP. The actual contrast is a user-dependent choice, whereas advantages and risks of the individual options are the same as for conventional MRI studies. For example, SSFP versions have to balance the potential for increased signal-to-noise ratio versus the occurrence of banding artifacts and the need for time-consuming shimming. So far, real-time MRI movies with T2/T1 contrast have been evaluated for TMJ studies using refocused FLASH sequences,[8,9] whereas fully balanced SSFP conditions have been demonstrated for cardiac MRI at 1.5 T[10] and 3.0 T.[11]

Real-Time MRI: Acquisition and Reconstruction

Real-time MRI data acquisition uses strongly undersampled radial gradient-echo sequences that use a turn-based sampling scheme that ensures spatial encoding by complementary sets of radial spokes in successive frames. Typically, the pattern repeats every 5 frames, although other schemes are possible. The present choice is motivated by experimental observations that a turn-based encoding scheme with temporal median filtering generates less residual streaking artifacts than a golden angle encoding scheme. On the other hand, golden angle trajectories may have advantages for model-based T1 mapping (see below).

Because radial encoding schemes densely sample the center of k-space, which originally was considered a drawback, such sequences are now particularly attractive for accelerated undersampled acquisitions as they best cover most of the relevant image information. Moreover, compared with spiral or echo-planar trajectories that involve prolonged echo trains, single-echo short-TE radial acquisitions represent a preferred choice because of their insensitivity to magnetic field inhomogeneities. In general, for any chosen field of view and spatial resolution, practical realizations use the highest possible bandwidth per pixel as well as the shortest possible echo time and repetition time to achieve the highest temporal resolution and to minimize off-resonance effects.

Preprocessing of real-time data involves a channel compression that is based on a principal component analysis. It serves to reduce the number of physical receive channels to a smaller number of virtual channels[12] (typically 10), which substantially reduces the computational demand without any noticeable loss in image quality. In addition, gradient delays are estimated during the preparatory phase of each

scan[13] and a corrected trajectory is applied for image reconstruction of the following acquisitions.

Serial image reconstruction is achieved by calibration-less parallel imaging using nonlinear inversion. Nonlinear inversion extends iterative SENSE[14] by formulating the image reconstruction as the solution to a nonlinear inverse problem. The strategy optimally exploits all available data to simultaneously estimate all complex-valued coil sensitivity maps and the complex-valued image.[15] Reconstructions of this ill-posed inverse problem are stabilized by regularization using prior knowledge. In particular, smoothness of the coil sensitivities is enforced by a suitable Sobolev norm, and the temporal redundancy in a time series (ie, the similarity of successive frames) is exploited by penalizing the difference to the previous frame.[6] Such conditions effectively constrain the iterative optimization and significantly enhance the usable degree of undersampling. It should be noted that many other types of temporal regularization techniques cannot be applied to real-time MRI because these methods need the data of a complete time series before starting image reconstruction.

Technically, the computation of a regularized solution to the nonlinear inverse problem is accomplished by the iteratively regularized Gauss-Newton method.[16] This method repeatedly solves a linearized regularized least squares problem in typically 6 to 7 iterations, whereas the regularization strength is typically reduced by a factor of 2 in each iterative step. Thus, in the final reconstruction, the regularization is very small, and the dominating data consistency term ensures temporal fidelity. The generic iteratively regularized Gauss-Newton method reconstruction framework can also be extended to include nonlinear physics-based models for parameter quantification as described below for phase-contrast flow MRI and T1 mapping.

Postprocessing of estimated images or maps differs depending on the specific application. For example, it may involve a multiplication of the resulting image with the root-sum-of-squares of the coil sensitivities to obtain an intensity profile similar to a fully sampled static reconstruction.[15] Residual undersampling artifacts (eg, streaks) can be removed by a temporal median filter with a window size adapted to the periodicity of the turn-based sampling scheme.[6] Finally, an edge-preserving spatial filter based on a modified nonlocal means filter is applied to improve the signal-to-noise ratio.[17] Temporal fidelity of the complete method is excellent as shown in phantom studies, but the median filter should not be used for the visualization of very fast movements of small objects.[18]

To achieve true real-time imaging, the reconstruction time per frame must be lower than the acquisition time. Therefore, a highly parallelized version of the algorithm was developed and implemented on a computer with multiple GPUs.[19] In brief, image reconstruction is based on a convolution of the image with the point-spread function that

TABLE 1. Exemplary acquisition parameters for selected real-time MRI studies

	Hand Movement	Dual-Slice TMJ	Speaking	Swallowing	Cardiac Function	Aortic Flow	CSF Flow
FOV, mm^2	192 × 192	128 × 128	192 × 192	192 × 192	320 × 320	320 × 320	192 × 192
Image matrix	256 × 256	170 × 170	136 × 136	148 × 148	200 × 200	212 × 212	256 × 256
Resolution, mm^2	0.75 × 0.75	0.75 × 0.75	1.4 × 1.4	1.3 × 1.3	1.6 × 1.6	1.5 × 1.5	0.75 × 0.75
Thickness, mm	4.0	6.0	8.0	8.0	6.0	6.0	5.0
TR, ms	3.85	2.21	2.22	2.10	1.96	2.56	5.68
TE, ms	2.30	1.35	1.47	1.33	1.22	1.70	4.61
Flip angle, degree	4	14	5	8	8	10	12
Spokes	13	2 × 21	9	19	17	2 × 5	2 × 11
Acquisition time, ms	50.0	2 × 50.0	20.0	40.0	33.3	2 × 12.8	2 × 62.5
Frame rate, s^{-1}	20	2 × 10	50	25	30	39	8

MRI indicates magnetic resonance imaging; TMJ, temporomandibular joint; CSF, cerebrospinal fluid; FOV, field of view; TR, repetition time; TE, echo time.

© 2019 The Author(s). Published by Wolters Kluwer Health, Inc.

can be implemented using a fast Fourier transform algorithm.[20] This requires only a single initial interpolation of the data onto a 2-fold oversampled grid, which is performed on the CPU as a preprocessing step. The iterative reconstruction itself then uses only the fast Fourier transform algorithm, point-wise operations, and scalar products that can be performed very efficiently on GPUs. By distributing the data of different receive channels or different frames to multiple GPUs, the reconstruction speed is increased even further.[21,22] Except for very large data matrices, most online reconstructions already run in real time with up to 50 frames per second (fps) and barely recognizable latency for the entire pipeline including visualization. Overall, the described real-time MRI technique is already suitable for interactive MRI-guided interventional procedures.[23]

Single-Shot T1 Mapping

Acquisition times on the order of tens of milliseconds allow for a direct monitoring of relaxation processes by real-time MRI. For example, serial images that sample the inversion-recovery (IR) process of the longitudinal magnetization after a single inversion pulse can be fitted pixel-wise to a physics-based signal model for quantitative T1 mapping. Such methods yield accurate T1 maps in only 4 seconds.[24] Improved versions can be obtained by integrating the IR signal model into the image reconstruction process[25,26] similar to and extending previous nonlinear model-based reconstruction methods for T2 mapping.[27] Both methods are also applicable to single-shot myocardial T1 mapping, for example, by selecting diastolic cardiac frames from a series of continuously acquired data during a 4-second breathhold.[28,29]

Real-Time Flow MRI

By extending the acquisition to 2 sets of images with different flow-encoding gradients, it is possible to perform phase-contrast flow MRI in real time. A first approach reconstructed respective pairs of images using the same coil sensitivities, and then computed the flow information by a pixel-wise phase difference of the 2 images in a postprocessing step.[30] The longer acquisition time needed for flow encoding can be ameliorated with the use of asymmetric gradient echoes.[31] Latest versions take advantage of an advanced model-based reconstruction[32] that jointly computes a magnitude image, all coil sensitivity maps, and a phase-difference (ie,

velocity) map directly from the raw data. The technique leads to reconstructions with higher spatiotemporal resolution as well as improved velocity maps with much reduced noise in image regions without signal support. The algorithm requires a careful tuning of scaling parameters, but recent advances solved this problem by performing this step automatically.[33]

RESULTS

Joint Movements

A natural candidate for dynamic imaging studies of nonperiodic processes that cannot be synchronized to an external reference signal are joint movements. So far, however, practical applications are somewhat limited by the standard design of MRI magnets, which requires examinations in supine or prone position and hampers movements of the shoulder or leg. On the other hand, current static MRI examinations of the ankle, knee, or shoulder reach superb quality, so that in most cases little add-on information is to be gained by real-time MRI. This situation may be different for patients who experience pain only during movement of a joint such as for example the hand or wrist. Figure 1 depicts selected coronal frames of a real-time MRI study of a healthy volunteer during right-left hand shaking. This study was motivated by patients complaining about persistent wrist pain during movement after healing of a bone fracture. The corresponding MRI movie (see Video, Supplemental Digital Content 1, http://links.lww.com/RLI/A444) has been recorded with a pair of thin flexible radiofrequency coil arrays (8 elements each) at 50 milliseconds resolution (20 fps) and relatively high spatial resolution (0.75 mm resolution, 4 mm slice thickness). The ability of real-time MRI studies to analyze clinical symptoms during actual movement promises to advance diagnostics in a number of joint problems.

Another clinically relevant application is the functional assessment of the TMJ, which is one of the important structures aiding in the opening and closing of the mouth during articulation, chewing, and swallowing. Temporomandibular disorders refer to an impaired functioning of the TMJ and frequently involve an abnormal disk-condyle relationship and pain. Figure 2 depicts selected frames (oblique sagittal views) of 2 real-time MRI movies of the right and left TMJ during a single voluntary opening of the mouth (0.75 mm resolution, 6 mm slice thickness). Effective delineation of the disk (bright structure) atop the mandibular
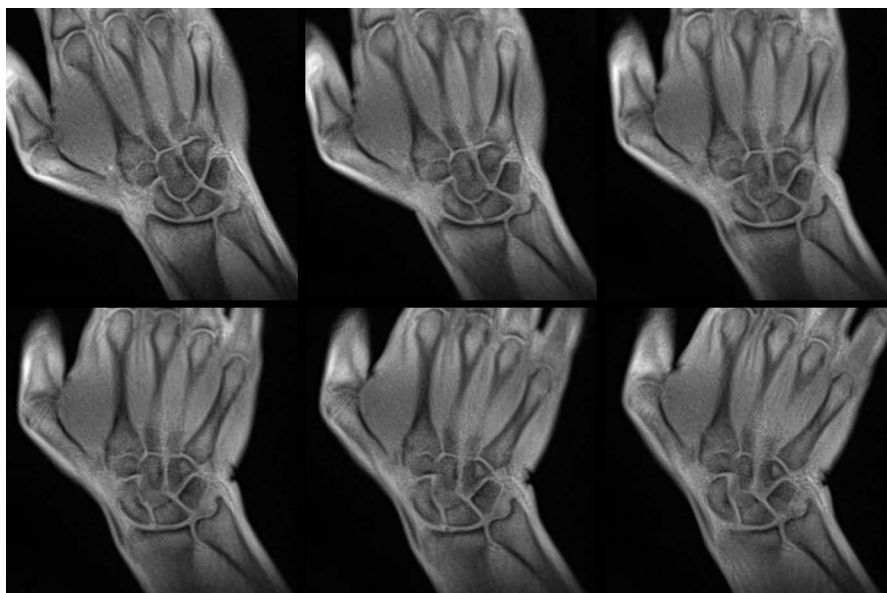

FIGURE 1. Wrist movement. Selected frames (coronal views from top left to bottom right) of a real-time MRI movie of the hand during left-right movement (50 milliseconds acquisition time, 0.75 mm resolution, 4 mm slice thickness). The frames are 40 images apart (2.0 seconds).
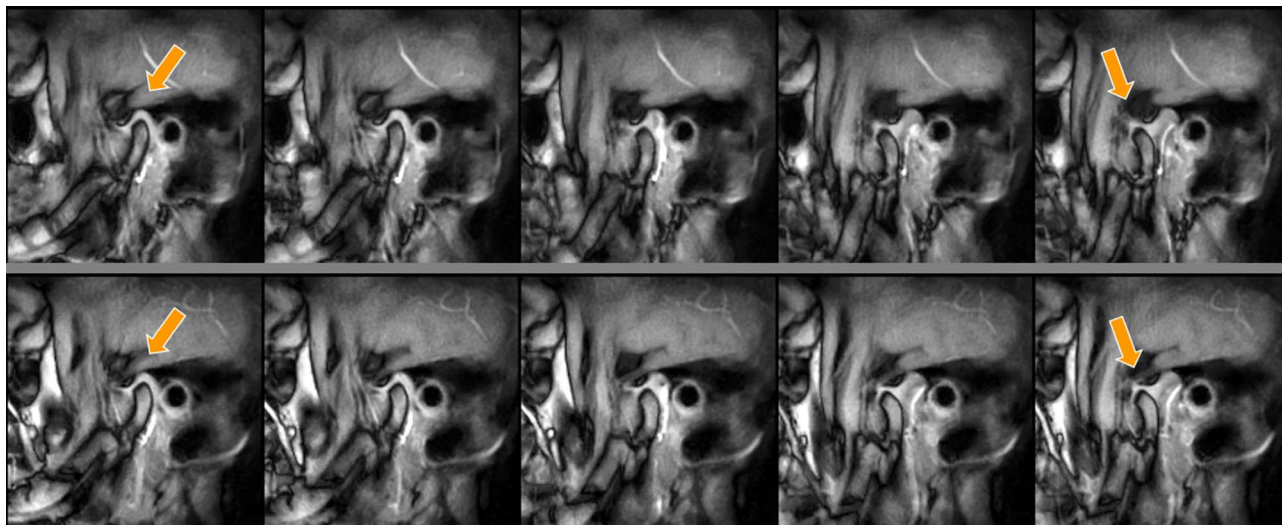
FIGURE 2. Temporomandibular joint. Selected frames (oblique sagittal views) of 2 simultaneous real-time MRI movies of the (top) right and (bottom) left temporomandibular joint during a single voluntary opening of the mouth (2 × 50 milliseconds acquisition time, 0.75 mm resolution, 6 mm slice thickness). The frames are 14 images apart (2.4 seconds) and cover the movement of the mandibular disk (bright structure, arrows) from a closed (left) to an open position (right).

condyle was achieved by T1-weighted images with opposed-phase water-fat contrast.[34] The frames in Figure 2 cover the movement of the disk from a closed (left) to an open mouth position (right). Extending previous work,[8,9] these results further improve the clinical versatility of real-time TMJ studies by the simultaneous recording of both movies (see Video, Supplemental Digital Content 2, http://links.lww.com/RLI/A445) in a frame-interleaved manner at 2 × 50 milliseconds resolution (2 × 10 fps). In fact, up to 4 simultaneous movies at 4 × 25 milliseconds resolution (4 × 10 fps) have been accomplished with clinically acceptable image quality.[34]

Articulation Studies

Real-time MRI is currently in use for the analysis of articulatory processes in different languages. Pertinent applications range from specific phonetic questions to disorders such as stuttering. For example, a special topic is the realization of vowel nasalization where the exact timing of tongue and velum is mandatory to control the respective air flow.[35] A typical real-time MRI movie of natural speaking with sound recording is shown in Video, Supplemental Digital Content 3, http://links.lww.com/RLI/A446, using a mid-sagittal plane of the head at a resolution of 20 milliseconds (50 fps). In these applications, high speed is required to resolve the rapid movements of the tongue tip. Similar arguments apply to studies of singing or whistling.

A related area that benefits from completely new insights by real-time MRI is brass playing.[36,37] An example of a simultaneous dual-slice recording of trombone playing in 2 orthogonal (ie, sagittal and coronal) sections is shown in Video, Supplemental Digital Content 4, http://links.lww.com/RLI/A447, at 2 × 20 milliseconds resolution (2 × 25 fps). Such studies already have a major influence on brass pedagogy as indicated by new textbooks[38] and Internet publications[39,40] about science-informed brass playing. These enterprises are further supported by the generation of a freely available MRI Brass Repository Project[41] that provides exemplary exercises of elite performers. A leading motivation is the observation that a significant proportion of professional brass musicians experiences focal task-specific dystonia.[42–44] An example is embouchure dystonia, which is characterized by the loss of control of facial and oral muscles while blowing air into the mouthpiece of a brass or wind instrument. These disorders can be devastating and often result in career termination, as abnormal muscle movements usually

create a reduction in performance quality. With current reconstruction speed, real-time MRI even allows for online visualization with negligible delay, which in turn offers visual feedback studies to self-control articulation processes while playing in the MRI magnet (unpublished results).

Swallowing and Beyond

Real-time MRI allows for dynamic studies of swallowing processes at high temporal resolution.[45] Such work includes diverse clinical aspects of esophageal transport and passage through the gastroesophageal junction. Current extensions evaluate the motility of the stomach and small bowel. Clinical interest focuses on disorders such as dysphagia[46] and gastroesophageal reflux disease[47,48] or the occurrence of hiatal hernia.[49] Figure 3 depicts selected midsagittal real-time MRI views of the oral cavity during a voluntary swallow of 5 mL pineapple juice at 40 milliseconds resolution (25 fps). The selected frames are 2 images apart (80 milliseconds) and cover the actual swallowing process (480 milliseconds) from initiation to esophageal transport. A full movie recording is shown in Video, Supplemental Digital Content 5, http://links.lww.com/RLI/A448.

The slow motility of the stomach muscular wall after filling (drinking water) is demonstrated in Figure 4 for an oblique plane along the long axis of the stomach. The images represent selected frames of a simultaneous triple-slice real-time MRI acquisition at 3 × 40 milliseconds resolution (3 × 8 fps). The frames are 3 × 30 images apart (3.6 seconds) and cover one full cycle of slow contractions and expansions. All 3 simultaneous real-time MRI movies are shown in Video, Supplemental Digital Content 6, http://links.lww.com/RLI/A449, which enhances the visibility of muscular contraction by accelerating the display to 40 fps.

Cardiac Function

T1-weighted real-time MRI of cardiac function at 3 T may be accomplished not only without electrocardiogram (ECG) gating and during free breathing, but also without additional shimming and the risk of SSFP banding artifacts.[11] Figures 5 and 6 reveal the typical image quality for a short-axis and 4-chamber view, respectively. The panels summarize 8 consecutive frames (266 milliseconds periods) of real-time MRI movies during postsystolic expansion at 33.3 milliseconds resolution (30 fps). Respective movies are shown in Videos, Supplemental Digital Content 7, http://links.lww.com/RLI/A450 and Supplemental Digital Content 8, http://links.lww.com/RLI/A451. If necessary, for
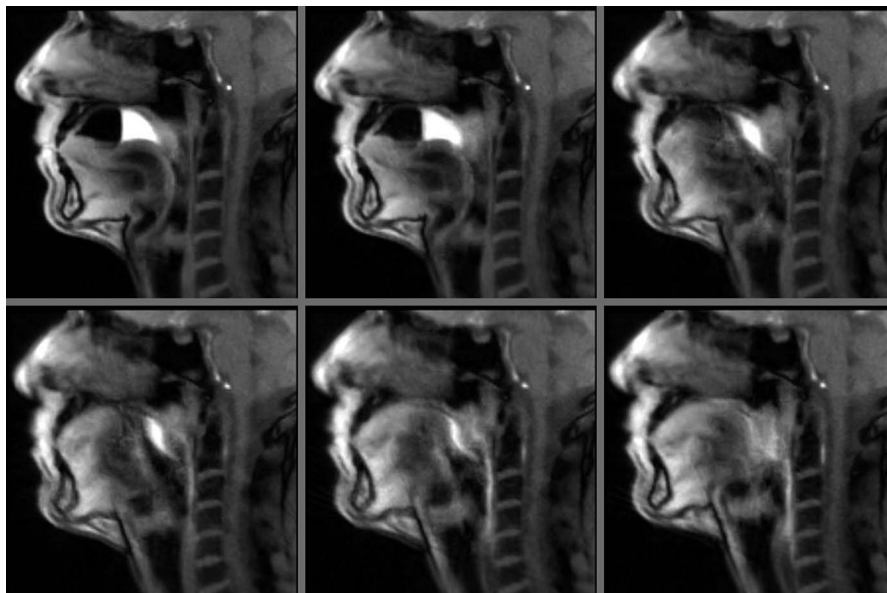
FIGURE 3. Swallowing. Selected frames (midsagittal views from top left to bottom right) of a real-time MRI movie of the oral cavity during a voluntary swallow of 5 mL pineapple juice (40 milliseconds acquisition time, 1.3 mm resolution, 8 mm slice thickness). The frames are 2 images apart (80 milliseconds) and cover the swallowing process (480 milliseconds) from initiation to esophageal transport.

example in young infants, even higher speed is possible such as 20 milliseconds or even 10 milliseconds resolution (ie, 50 to 100 fps). Other practical variants are sequential movie recordings in multiple sections, which cover the entire volume of the heart in, for example, 1 minute when acquiring 15 real-time MRI movies of 4 seconds duration each.

Real-time cardiac MRI obviously allows for improved access to patients with arrhythmias such as atrial fibrillation as each individual heartbeat becomes functionally available. This further offers new diagnostic opportunities when analyzing the immediate functional responses to stress, breathing maneuvers, or physical exercise[11] ("online physiology"). On the other hand, the already achievable speed for

online reconstruction allows for interactive real-time cardiac MRI using the same spatiotemporal resolution as used for the data shown in Figures 5 and 6 or Videos, Supplemental Digital Content 7 http://links.lww.com/RLI/A450 and Supplemental Digital Content 8, http://links.lww.com/RLI/A451. A corresponding example is shown in Video, Supplemental Digital Content 9, http://links.lww.com/RLI/A452, which represents a video recording of the MRI console, while interactively changing the slice position during real-time MRI at 30 fps. Without specific clinical question, the chosen example simply demonstrates the future potential of high-quality real-time MRI to monitor minimally invasive interventional procedures.[23] Future applications will further
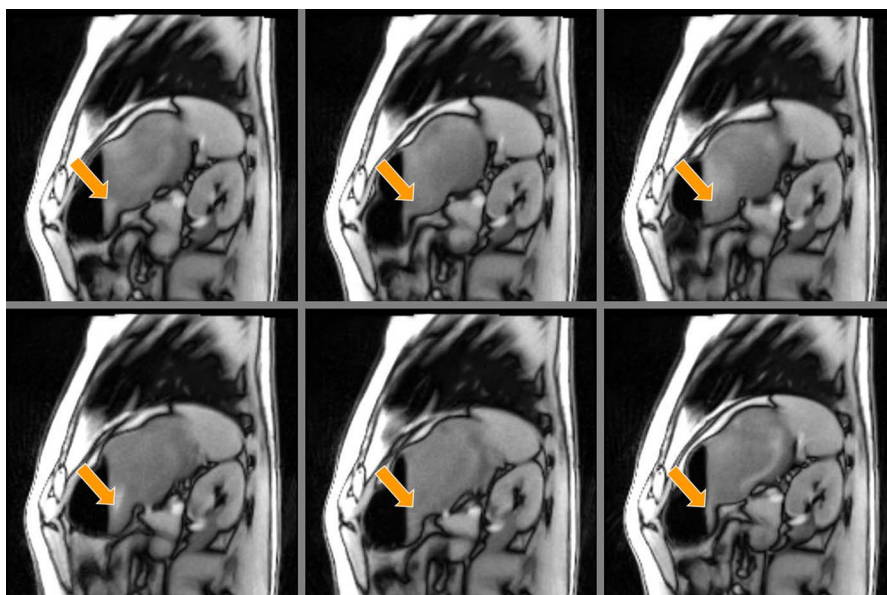

FIGURE 4. Stomach motility. Selected frames (oblique views from top left to bottom right, same section) of a simultaneous triple-slice real-time MRI acquisition of the movements of the muscular wall (3×40 milliseconds acquisition time, 1.5 mm resolution, 8 mm slice thickness). The frames are 3×30 images apart (3.6 seconds) and cover one cycle of slow contractions and expansions (see arrows).
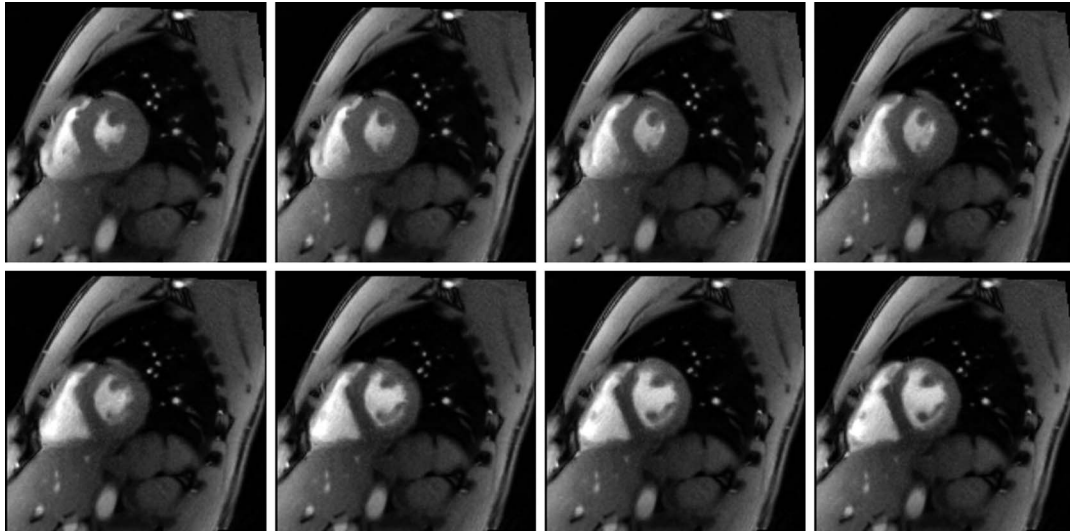
FIGURE 5. Cardiac function—short-axis view. Consecutive frames (top left to bottom right, 266 milliseconds period) of a real-time MRI movie of the heart covering postsystolic expansion during free breathing and without ECG gating (33.3 milliseconds acquisition time, 1.6 mm resolution, 6 mm slice thickness).

benefit from the ability to not only change the slice position dynamically, but also to modify other experimental parameters that, for example, control the spatiotemporal resolution and image contrast.

Blood Flow and Cerebrospinal Fluid Dynamics

Quantitative determinations of blood flow are essential elements of a comprehensive cardiovascular MRI examination. Real-time MRI therefore has been extended to phase-contrast through-plane flow studies, which rely on 2 acquisitions of differentially flow-encoded datsets.[30,31] More recently, such applications have considerably been improved by the adaptation of a model-based reconstruction technique.[32,33] Model-based real-time flow MRI directly calculates an anatomic image and a phase-contrast velocity map as well as all coil sensitivity maps from the respective raw datasets. The approach achieves flow maps at much improved spatiotemporal resolution and with almost no noise as it completely avoids the complex subtraction of separately calculated phase images. An example is shown in Figure 7 that summarizes 8 consecutive postsystolic frames (205 milliseconds period from high to low flow) of a real-time phase-contrast flow MRI movie of the ascending and descending aorta during free breathing and without ECG gating at 25.6 milliseconds resolution (39 fps). The corresponding real-time MRI movie is shown in Video, Supplemental Digital Content 10, http://links.lww.com/RLI/A453.

Similar to real-time cardiac MRI also flow quantification benefits from access to individual heartbeats and the immediate functional response to a physical challenge such as a Valsalva or Mueller breathing maneuver.[50,51] Moreover, the principle capability to monitor flow phenomena that are not linked to period cardiac processes now offers studies without "prejudice" due to ECG gating. This not only applies to venous blood flow in peripheral vessels[52] or in the vena cava but also to the dynamics of the cerebrospinal fluid (CSF). In the latter case, real-time MRI[53] and real-time phase-contrast flow MRI[54] unambiguously identified inspiration as the dominant factor regulating CSF flow during forced
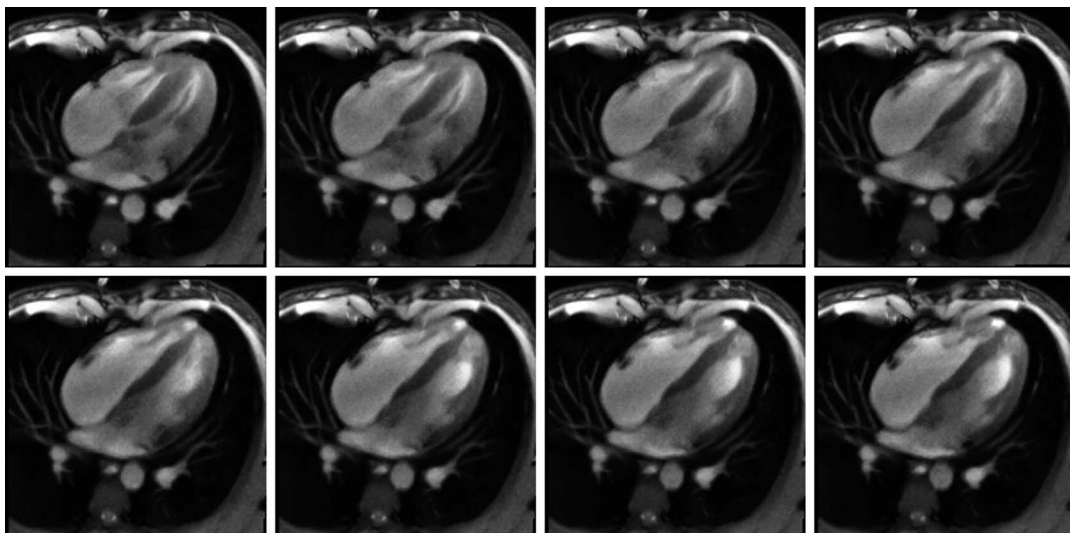

FIGURE 6. Cardiac function—4-chamber view. Consecutive frames (top left to bottom right, 266 milliseconds period) of a real-time MRI movie of the heart covering postsystolic expansion during free breathing and without ECG gating (33.3 milliseconds acquisition time, 1.6 mm resolution, 6 mm slice thickness).
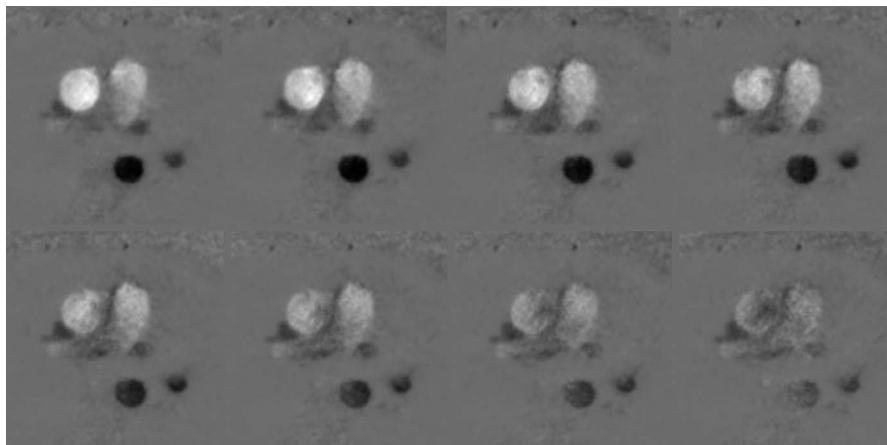
FIGURE 7. Quantitative velocity maps of aortic blood flow. Consecutive postsystolic frames (top left to bottom right, 179 milliseconds period) of a real-time phase-contrast flow MRI movie of the ascending and descending aorta during free breathing and without ECG gating (25.6 milliseconds acquisition time, 1.5 mm resolution, 6 mm slice thickness). Rather than taking a complex phase difference, the images were obtained by a model-based reconstruction, which jointly estimates an anatomical image, a velocity map, and all coil sensitivity maps directly from the raw data.

breathing. Figure 8 depicts 8 consecutive velocity maps (1000 milliseconds period) obtained by real-time phase-contrast MRI of CSF dynamics in the cervical spinal canal during French horn playing at 125 milliseconds resolution (8 fps). During inspiration, CSF moves upwards (bright signal, orange arrows), whereas exhalation causes a downward flow (dark signal, yellow arrows), respectively. The observation of upward CSF flow into the head and brain in response to forced inspiration counterbalances the inspiratory-regulated venous outflow out of the head/neck region, which is caused by the reduced intrathoracic pressure during deep inspiration. Thus, CSF and venous blood flow are tightly interconnected and balanced to ensure a constant intracranial volume and pressure. A complete movie with sound recording of both anatomic images and velocity maps is shown in Video, Supplemental Digital Content 11, http://links.lww.com/RLI/A454.

Single-Shot T1 Mapping

Real-time MRI acquisitions may further be exploited for high-quality single-shot T1 mapping by covering a single IR process by continuous acquisitions after an initial inversion radiofrequency pulse. Serial image reconstruction may then be followed by pixel-wise fitting of the IR signal model.[24,28] A corresponding example is shown in Figure 9 for selected T1 maps of the human brain, each acquired within 4 seconds at 0.5 mm in-plane resolution. The diagnostic potential of rapid high-resolution T1 mapping was recently demonstrated in patients with cervical spinal cord compression who revealed significantly decreased T1 relaxation times of the compressed spinal cord—even for a grade I stenosis—in comparison to unaffected segments above and below.[55]

In terms of methodology, the acquisition and reconstruction of a large number of serial images during IR hints to significant redundancy as only very few parametric maps are required to describe the IR signal model. This problem may be taken care of by a model-based reconstruction technique that integrates the IR signal model directly into the nonlinear inverse reconstruction process.[25,26] Figure 10 presents diastolic T1 maps of the human heart of 6 subjects obtained by single-shot IR FLASH (4 seconds measuring time each during a breath hold). The method uses a small golden angle radial trajectory, automatically
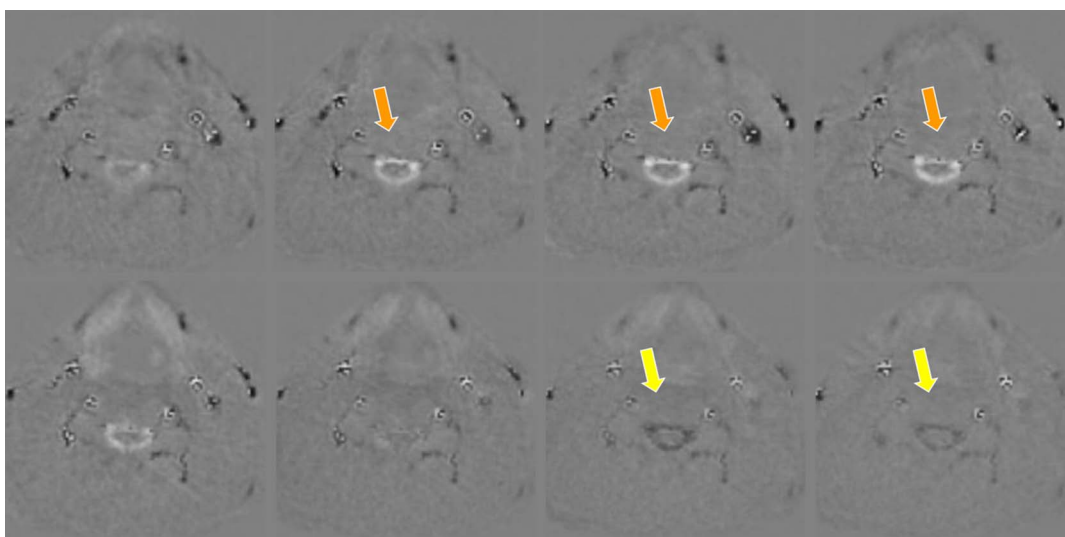

FIGURE 8. Quantitative velocity maps of CSF dynamics (model-based reconstruction as in Fig. 7). Consecutive frames (top left to bottom right, 1000 milliseconds period) of a real-time phase-contrast flow MRI movie of CSF flow in the cervical spinal canal during French horn playing (125 milliseconds acquisition time, 0.75 mm resolution, 5 mm slice thickness). During inspiration, CSF moves upwards (bright signal, orange arrows), whereas subsequent exhalation causes a downward flow (dark signal, yellow arrows), respectively.
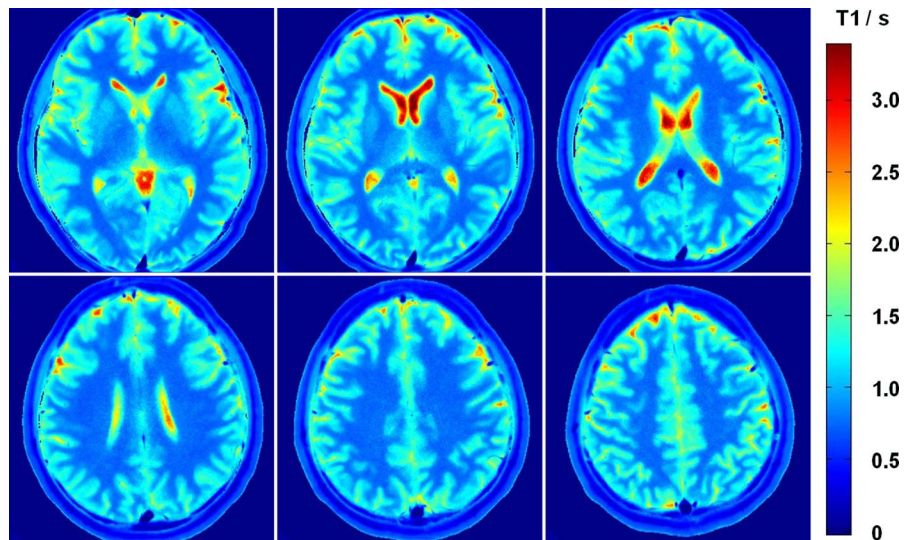
FIGURE 9. T1 maps of the human brain (same subject) obtained by single-shot inversion-recovery radial FLASH (4 seconds) and subsequent pixel-wise fitting (65 milliseconds acquisition time per frame, 0.5 mm resolution, 4 mm slice thickness).

deletes systolic frames, and performs a model-based reconstruction with L1 sparsity constraint.[29] To reduce the computational burden and memory allocation, the data are binned to 45 milliseconds acquisitions. Such applications may easily be extended to other abdominal organs such as liver, spleen, and kidney.

DISCUSSION

Based on numerous applications in science and medicine, the proposed method for real-time MRI emerges as a robust and versatile tool for dynamic monitoring of arbitrary physiological processes and body functions. Moreover, practical implementations may be realized as upgrades (hardware and software) to commercial MRI systems and thus allow for online acquisition, reconstruction, visualization, and storage of images with negligible delay.[56] Nevertheless, at this stage, the lack of general availability must be considered a major limitation, which so far precludes the planning of more extended clinical trials. This is because of

the need for an additional GPU computer to overcome the limitations of current commercial MRI systems and meet the high computational demand (and memory demand for model-based versions).

Another issue is field strength. Although 1.5-T studies are certainly possible and should be further explored, at this stage, a preferred option is the use of a high-field (3.0 T) MRI system. This is mainly because short-TE real-time MRI sequences fully benefit from the increased nuclear polarization—and in some cases also from better gradient capabilities and more sophisticated radiofrequency coil arrays. A practical concern for cardiovascular real-time MRI is the availability of suitable postprocessing software to deal with large series of, for example, hundreds of images that cover multiple heart beats and respiratory cycles.

A final remark addresses a plurality of alternative strategies to real-time imaging that attempt to accelerate conventional MRI procedures. In this context, it should be noted that parallel imaging techniques with reconstructions by SENSE,[4,14] GRAPPA,[5,57] and compressed sensing[58] only solve a linear inverse problem. To be generally applicable, such
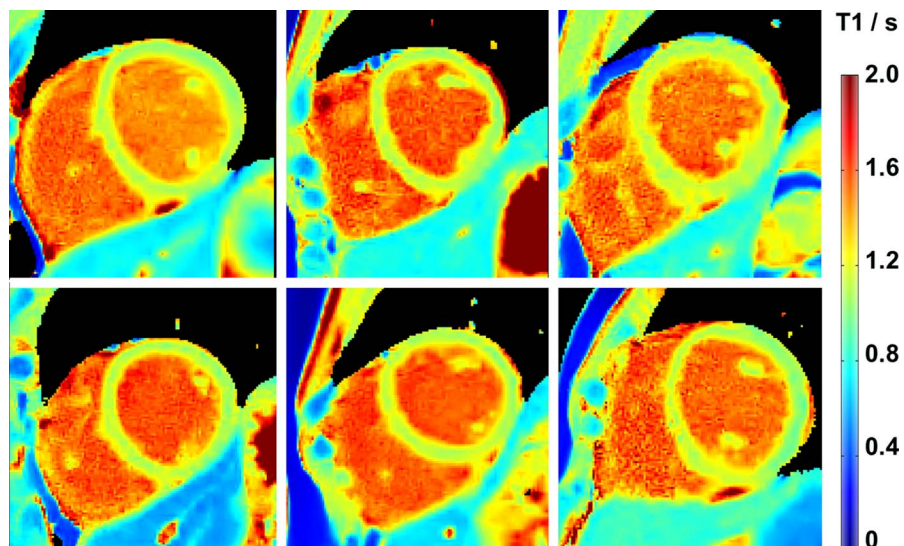

FIGURE 10. T1 maps of the human heart (6 subjects) obtained by single-shot inversion-recovery radial FLASH (4 seconds) with automatic deletion of systolic frames and model-based reconstruction with L1 sparsity constraint (45 milliseconds data binning, 1.0 mm resolution, 8 mm slice thickness).

approaches therefore require additional information (eg, predetermined coil sensitivity maps) for reducing the number of unknowns during iterative optimization to one, that is, to linearize the nonlinear inverse problem. On the other hand, clinical demands do not always ask for cross-sectional imaging in real time, but often prefer slower though accelerated scans of a larger volume. Typical examples are dynamic contrast-enhanced MRI studies of the breast[59–61] and liver,[62–64] which have recently been performed by diverse combinations of parallel imaging, encoding trajectories, and compressed sensing. Whether similar applications may be realized by adopting the principles of real-time MRI as described here remains to be seen. However, preliminary trials to achieve rapid motion-robust volume coverage by exploiting spatial rather than temporal similarity turn out to be very promising (unpublished results).

Taken together, the main obstacle for a more frequent use of real-time MRI is not the lack of a technical solution, but the limited availability of suitable MRI scanners and the corresponding lack of clinical experience, which can only be gained by many more patient-oriented research studies. Without sufficient medical evidence and without newly established clinical standards, there may be practical resistance to abandon MRI techniques that have been used for up to 3 decades such as ECG-gated procedures in cardiovascular examinations. Without doubt, future MRI-based radiology needs to step ahead and in many fields of application deserves a change of paradigm.

ACKNOWLEDGMENTS

REFERENCES

1. Frahm J, Haase A, Matthaei D. Rapid NMR imaging of dynamic processes using the FLASH technique. *Magn Reson Med*. 1986;3:321–327.
2. Mansfield P. Multi-planar image formation using NMR spin echoes. *J Phys C: Solid State Phys*. 1977;10:L55–L58.
3. Ahn CB, Kim JH, Cho ZH. High-speed spiral-scan echo planar NMR imaging. *IEEE Trans Med Imaging*. 1986;5:2–7.
4. Pruessmann KP, Weiger M, Scheidegger MB, et al. SENSE: sensitivity encoding for fast MRI. *Magn Reson Med*. 1999;42:952–962.
5. Sodickson DK, Manning WJ. Simultaneous acquisition of spatial harmonics (SMASH): fast imaging with radiofrequency coil arrays. *Magn Reson Med*. 1997;38:591–603.
6. Uecker M, Zhang S, Voit D, et al. Real-time MRI at a resolution of 20 ms. *NMR Biomed*. 2010;23:986–994.
7. Roeloffs VB, Voit D, Frahm J. Spoiling without additional gradients—radial FLASH MRI with randomized radiofrequency phases. *Magn Reson Med*. 2016; 75:2094–2099.
8. Krohn S, Gersdorff N, Wassmann T, et al. Real-time MRI of the temporomandibular joint at 15 frames per second—a feasibility study. *Eur J Radiol*. 2016;85: 2225–2230.
9. Krohn S, Frahm J, Merboldt KD, et al. Diagnosis of disk displacement using real-time MRI: clinical report of two patients. *J Prosthet Dent*. 2018;119: 206–209.
10. Voit D, Zhang S, Unterberg-Buchwald C, et al. Real-time cardiovascular magnetic resonance at 1.5 T using balanced SSFP and 40 ms resolution. *J Cardiovasc Magn Reson*. 2013;15:79.
11. Zhang S, Joseph AA, Voit D, et al. Real-time MRI of cardiac function and flow–recent progress. *Quant Imaging Med Surg*. 2014;4:313–329.
12. Huang F, Vijayakumar S, Li Y, et al. A software channel compression technique for faster reconstruction with many channels. *Magn Reson Imaging*. 2008;26: 133–114.
13. Block KT, Uecker M. Simple method for adaptive gradient-delay compensation in radial MRI. Annual Meeting ISMRM, Montreal 2011. *Proc Intl Soc Mag Reson Med*. 2011;19:2816.
14. Pruessmann KP, Weiger M, Börnert P, et al. Advances in sensitivity encoding with arbitrary k-space trajectories. *Magn Reson Med*. 2001;46:638–651.
15. Uecker M, Hohage T, Block KT, et al. Image reconstruction by regularized nonlinear inversion—joint estimation of coil sensitivities and image content. *Magn Reson Med*. 2008;60:674–682.
16. Bakushinsky AB, Kokurin MY. *Iterative Methods for Approximate Solution of Inverse Problems*. Dordrecht, the Netherlands: Springer; 2005.
17. Klosowski J, Frahm J. Image denoising for real-time MRI. *Magn Reson Med*. 2017;77:1340–1352.
18. Frahm J, Schätz S, Untenberger M, et al. On the temporal fidelity of nonlinear inverse reconstructions for real-time MRI—the motion challenge. *The Open Med Imaging J*. 2014;8:1–7.
19. Uecker M, Zhang S, Frahm J. Nonlinear inverse reconstruction for real-time MRI of the human heart using undersampled radial FLASH. *Magn Reson Med*. 2010; 63:1456–1462.
20. Wajer F, Pruessmann KP. Major speedup of reconstruction for sensitivity encoding with arbitrary trajectories. Annual Meeting of the ISMRM, Glasgow 2001. *Proc Intl Soc Mag Reson Med*. 2001;9:767.
21. Schaetz S, Uecker M. A multi-GPU programming library for real-time applications. In: Xiang Y, Stojmenovic I, Apduhan BO, et al., eds. *Algorithms and Architectures for Parallel Processing. ICA3PP 2012. Lecture Notes in Computer Science* vol. 7439. Berlin, Germany: Springer; 2012:114–128.
22. Schaetz S, Voit D, Frahm J, et al. Accelerated computing in magnetic resonance imaging: real-time imaging using nonlinear inverse reconstruction. *Comp Math Methods Med*. 2017;2017:3527269.
23. Unterberg-Buchwald C, Ritter CO, Reupke V, et al. Targeted endomyocardial biopsy guided by real-time magnetic resonance imaging. *J Cardiovasc Magn Reson*. 2017;19:45.
24. Wang X, Roeloffs VB, Merboldt KD, et al. Single-shot multi-slice T1 mapping at high spatial resolution—inversion-recovery FLASH with radial undersampling and iterative reconstruction. *The Open Med Imaging J*. 2015;9:1–8.
25. Roeloffs VB, Wang X, Sumpf T, et al. Model-based reconstruction for T1 mapping using single-shot inversion-recovery radial FLASH. *Int J Imaging Syst Techn*. 2016;26:254–263.
26. Wang X, Roeloffs VB, Klosowski J, et al. Model-based T1 mapping with sparsity constraints using single-shot inversion-recovery radial FLASH. *Magn Reson Med*. 2018;79:730–740.
27. Block KT, Uecker M, Frahm J. Model-based iterative reconstruction for radial fast spin-echo MRI. *IEEE Trans Med Imaging*. 2009;28:1759–1769.
28. Wang X, Joseph AA, Kalentev O, et al. High-resolution myocardial T1 mapping using single-shot inversion-recovery fast low-angle shot MRI with radial undersampling and iterative reconstruction. *Br J Radiol*. 2016;89:20160255.
29. Wang X, Kohler F, Unterberg-Buchwald C, et al. Model-based myocardial T1 mapping with sparsity constraints using single-shot inversion-recovery radial FLASH. *J Cardiovasc Magn Reson*. 2019. In press.
30. Joseph AA, Kowallick JT, Merboldt KD, et al. Real-time flow MRI of the aorta at a resolution of 40 ms. *J Magn Reson Imaging*. 2014;40:206–213.
31. Untenberger M, Tan Z, Voit D, et al. Advances in real-time phase-contrast flow MRI using asymmetric radial gradient echoes. *Magn Reson Med*. 2016;75: 1901–1908.
32. Tan Z, Roeloffs VB, Voit D, et al. Model-based reconstruction for real-time phase-contrast flow MRI—improved spatiotemporal accuracy. *Magn Reson Med*. 2017; 77:1082–1093.
33. Tan Z, Hohage T, Kalentev O, et al. An eigenvalue approach for the automatic scaling of unknowns in model-based reconstructions: application to real-time phase-contrast flow MRI. *NMR Biomed*. 2017. [Epub ahead of print].
34. Krohn S, Joseph AA, Voit D, et al. Multi-slice real-time MRI of temporomandibular joint dynamics. *Dentomaxillofac Radiol*. 2018;20180162.
35. Niebergall A, Zhang S, Kunay E, et al. Real-time MRI of speaking at a resolution of 33 ms: undersampled radial FLASH with nonlinear inverse reconstruction. *Magn Reson Med*. 2012;69:477–485.
36. Iltis PW, Schoonderwaldt E, Zhang S, et al. Real-time MRI comparisons of brass players: a methodological pilot study. *Hum Mov Sci*. 2015;42:132–145.
37. Iltis PW, Frahm J, Voit D, et al. High-speed real-time MRI of fast tongue movements in elite horn players. *Quant Imaging Med Surg*. 2015;5:374–381.
38. Epstein E. *Horn Playing from the Inside Out. A Method for All Brass Musicians*. 3rd ed. Brookline, MA: Eli Epstein Productions; 2016.
39. Yeo D. Seeing the Unseen: Trombone Playing Through the Eye of a MRI Scanner. 2017. Available at: https://thelasttrombone.com/2017/08/22/seeing-the-unseen-trombone-playing-through-the-eye-of-a-mri-scanner-with-the-mri-brass-repository-project/.
40. Willis S. Music and Science. *Deutsche Welle*. 2015. Available at: https://sarah-willis.com/episodes/15-music-and-science/.

41. Iltis PW. Magnetic Resonance Imaging and Horn Playing: The MRI Horn Repository Project. Available at: https://www.hornsociety.org/index.php?option=com_content&view=article&id=1083:mri-iltis&catid=295:newsletter&Itemid=417.

42. Iltis PW, Frahm J, Voit D, et al. Divergent oral cavity motor strategies between healthy elite and dystonic horn players. *J Mov Dis*. 2015;2:15.

43. Iltis PW, Frahm J, Voit D, et al. Inefficiencies in motor strategies of horn players with embouchure dystonia: comparisons to elite performers. *Med Probl Perform Art*. 2016;31:69–77.

44. Douglass N, Iltis PW, Frahm J, et al. Remediating abnormal oral cavity motor strategies in a horn player using RT-MRI: a case study. *Int J Orofacial Myology*. 2017;43:5–17.

45. Olthoff A, Zhang S, Schweizer R, et al. On the physiology of normal swallowing as revealed by magnetic resonance imaging in real time. *Gastrointest Res Pract*. 2014;2014:493174.

46. Olthoff A, Carstens PO, Zhang S, et al. Evaluation of dysphagia by novel real-time MRI. *Neurology*. 2016;87:1–7.

47. Zhang S, Joseph AA, Gross L, et al. Diagnosis of gastroesophageal reflux disease using real-time magnetic resonance imaging. *Sci Rep*. 2015;5:12112.

48. Seif Amir Hosseini A, Beham A, Uhlig J, et al. Intra- and interobserver variability in the diagnosis of GERD by real-time MRI. *Eur J Radiol*. 2018;104:14–19.

49. Seif Amir Hosseini A, Uhlig J, Streit U, et al. Real-time MRI for the dynamic assessment of fundoplication failure in patients with gastroesophageal reflux disease. *Eur Radiol*. 2019. [Epub ahead of print].

50. Kowallick JT, Joseph AA, Unterberg-Buchwald C, et al. Real-time phase-contrast flow MRI of the ascending aorta and superior vena cava as a function of intrathoracic pressure (Valsalva maneuvre). *Br J Radiol*. 2014;87:20140401.

51. Fasshauer M, Joseph AA, Kowallick JT, et al. Real-time phase-contrast flow MRI of hemodynamic changes in the ascending aorta and superior vena cava during Mueller maneuver. *Clin Radiol*. 2014;69:1066–1071.

52. Joseph AA, Merboldt KD, Voit D, et al. Real-time magnetic resonance imaging of deep venous flow during muscular exercise-preliminary experience. *Cardiovasc Diagn Ther*. 2016;6:473–481.

53. Dreha-Kulaczewski S, Joseph AA, Merboldt KD, et al. Inspiration is the major regulator of human CSF flow. *J Neurosci*. 2015;35:2485–2491.

54. Dreha-Kulaczewski S, Joseph AA, Merboldt KD, et al. Identification of the upward movement of human CSF in vivo and its relation to the brain venous system. *J Neurosci*. 2017;37:2395–2402.

55. Maier IL, Hofer S, Joseph AA, et al. Quantification of spinal cord compression using T1 mapping in patients with cervical spinal canal stenosis—preliminary experience. *NeuroImage Clin*. 2019;21:101639.

56. For availability, contact the corresponding author Dr Jens Frahm, Biomedizinische NMR, Max-Planck-Institut für Biophysikalische Chemie, 37070 Göttingen, Germany.

57. Griswold MA, Jakob PM, Heidemann RM, et al. Generalized autocalibrating partially parallel acquisitions (GRAPPA). *Magn Reson Med*. 2002;47:1202–1210.

58. Lustig M, Donoho D, Pauly JM. Sparse MRI: the application of compressed sensing for rapid MR imaging. *Magn Reson Med*. 2007;58:1182–1195.

59. Benkert T, Block KT, Heller S, et al. Comprehensive dynamic contrast-enhanced 3D magnetic resonance imaging of the breast with fat/water separation and high spatiotemporal resolution using radial sampling, compressed sensing, and parallel imaging. *Invest Radiol*. 2017;52:583–589.

60. Morrison CK, Henze Bancroft LC, DeMartini WB, et al. Novel high spatiotemporal resolution versus standard-of-care dynamic contrast-enhanced breast MRI: comparison of image quality. *Invest Radiol*. 2017;52:198–205.

61. Vreemann S, Rodriguez-Ruiz A, Nickel D, et al. Compressed sensing for breast MRI: resolving the trade-off between spatial and temporal resolution. *Invest Radiol*. 2017;52:574–582.

62. Kaltenbach B, Bucher AM, Wichmann JL, et al. Dynamic liver magnetic resonance imaging in free-breathing: feasibility of a Cartesian T1-weighted acquisition technique with compressed sensing and additional self-navigation signal for hard-gated and motion-resolved reconstruction. *Invest Radiol*. 2017;52:708–714.

63. Yoon JH, Yu MH, Chang W, et al. Clinical feasibility of free-breathing dynamic T1-weighted imaging with Gadoxetic Acid-enhanced liver magnetic resonance imaging using a combination of variable density sampling and compressed sensing. *Invest Radiol*. 2017;52:596–604.

64. Yoon JH, Lee JM, Yu MH, et al. Evaluation of transient motion during Gadoxetic Acid-enhanced multiphasic liver magnetic resonance imaging using free-breathing Golden-Angle radial sparse parallel magnetic resonance imaging. *Invest Radiol*. 2018;53:52–61.